

## Measuring thin film and multilayer elastic constants by coupling *in situ* tensile testing with x-ray diffraction

K. F. Badawi, P. Villain,<sup>a)</sup> Ph. Goudeau, and P.-O. Renault

Laboratoire de Métallurgie Physique, UMR 6630 CNRS/Université de Poitiers, SP2MI, BP 30179, 86962 Futuroscope Chasseneuil Cedex, France

(Received 28 January 2002; accepted for publication 30 April 2002)

A direct determination of the Young's modulus and the Poisson's ratio in a 140 nm polycrystalline tungsten thin film deposited by ion-beam sputtering on a polyimide substrate has been performed by coupling x-ray diffraction measurements with *in situ* tensile testing. The method described in this article to extract the Young's modulus of thin films from the evolution of the  $\sin^2 \psi$  curves as a function of applied load only requires to know the substrate Young's modulus. The determination of the thin film Poisson's ratio can be realized without knowing any of the substrate elastic constants. In the case of the tungsten thin film, the obtained Young's modulus was close to the bulk material one whereas the Poisson's ratio was significantly larger than the bulk one. © 2002 American Institute of Physics. [DOI: 10.1063/1.1488701]

There has been an increasing interest about the mechanical properties of thin films. Literature data show clearly that the elastic properties of metallic thin films and multilayers can differ significantly from the bulk metal ones.<sup>1-3</sup> In previous articles,<sup>4-6</sup> we presented a graphical method (called the "intersection method") to extract the Poisson's ratio in thin films or multilayers deposited on substrates from the evolution of the  $\sin^2 \psi$  curves as a function of the applied strain. This method had knowledge of the substrate Poisson's ratio.

In this letter, we describe a more accurate analytical method. It determines the Poisson's ratio of a supported thin film without using any of the elastic constants of the substrate, thus the Poisson's ratio of the thin film can be obtained even if the substrate is unknown. Concerning the Young's modulus of the thin film, the only data to know is the Young's modulus of the substrate. This method is based on the " $\sin^2 \psi$  method" which has already been extensively described elsewhere.<sup>7,8</sup> It consists of applying a uniaxial tensile force to the sample *in situ* in an x-ray diffractometer. The thin film elastic constants are determined by studying the evolution of the  $\sin^2 \psi$  curves as a function of the applied load. The main assumption in the following calculations is the elastic and linear behavior of both the substrate and the thin film.

Using x-ray diffraction, the strain  $\varepsilon_{\phi\psi}$  measured in the direction  $\mathbf{e}_{\phi\psi}$  defined in the specimen coordinate system ( $\mathbf{e}_{11}$ ,  $\mathbf{e}_{22}$ ,  $\mathbf{e}_{33}$ ) by the two Euler angles  $\phi$  and  $\psi$  (Fig. 1) is given by

$$\varepsilon_{\phi\psi} = \ln \left( \frac{d_{\phi\psi}}{d_0} \right) = \ln \left( \frac{\sin \theta_0}{\sin \theta} \right), \quad (1)$$

where  $d_{\phi\psi}$  (resp.  $d_0$ ) is the (resp. unstrained) lattice plane spacing of the  $\{hkl\}$  planes,  $\theta_{\phi\psi}$  and  $\theta_0$  the angular positions of the corresponding diffraction peaks through Bragg's law.

For the polycrystalline specimen with a random crystalline orientation and negligible shear stress and stress gradient in the x-ray depth probed, the strain  $\varepsilon$  depends linearly upon  $\sin^2 \psi$ ,  $\psi$  being the angle between the normal to the diffracting planes and the sample surface normal. In particular for  $\phi = 0$ :

$$\varepsilon_{0,\psi} = (\varepsilon_{11} - \varepsilon_{33}) \sin^2 \psi + \varepsilon_{33}. \quad (2)$$

Then, for an elastic isotropic material, Hooke's laws give the linear relationships between the strains and stresses via the Young's modulus and Poisson's ratio.

The tensile tester supporting the sample is placed at the center of the goniometer so that the loading direction corresponds to the  $\mathbf{e}_{11}$  sample axis. Assuming a uniaxial applied stress state ( $\sigma_{22}^{Af} = \sigma_{33}^{Af} = 0$ ), the stress  $\sigma_{11}^{Af}$  applied to the thin film is related to the load  $F$  by

$$\sigma_{11}^{Af} = \frac{F}{b \left( e_f + e_s \frac{E_s}{E_f} \right)}, \quad (3)$$

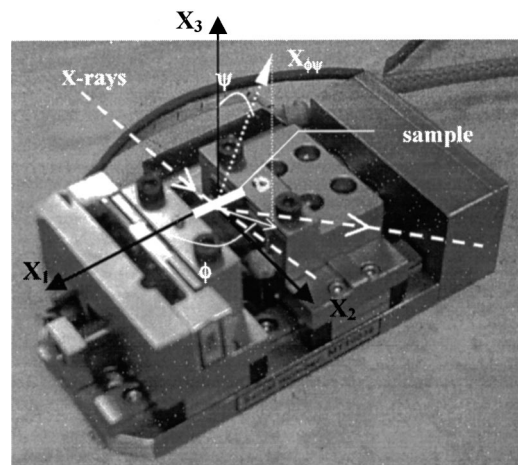


FIG. 1. Deben™ tensile tester with the sample coordinate ( $X_1$ ,  $X_2$ ,  $X_3$ ) and the x-ray measurement direction  $X_{\phi\psi}$ .

<sup>a)</sup> Author to whom correspondence should be addressed; electronic mail: pascalle.villain@etu.univ-poitiers.fr

where  $b$  is the sample width,  $e_f$  (resp.  $e_s$ ) the film (resp. substrate) thickness, and  $E_f$  (resp.  $E_s$ ) the thin film (resp. substrate) Young's modulus. Then, combining relations (1), (2), and (3), we obtain the following equation for a given  $\{hkl\}$  plane family:

$$\ln\left(\frac{1}{\sin\theta_\psi}\right) = P_1^f \sin^2\psi + m_1^f,$$

with

$$P_1^f = \left(\frac{1 + \nu_f}{E_f}\right)(\sigma_{11}^{Af} + \sigma_{11}^{rf})$$

$$= \left(\frac{1 + \nu_f}{E_s e_s + E_f e_f}\right) \frac{F}{b} + \left(\frac{1 + \nu_f}{E_f}\right) \sigma_{11}^{rf},$$

and

$$m_1^f = -\frac{\nu_f}{E_f}(\sigma_{11}^{Af} + \sigma_{22}^{Af} + \sigma_{11}^{rf} + \sigma_{22}^{rf}) + \ln\left(\frac{1}{\sin\theta_0}\right)$$

$$= \left(\frac{-\nu_f}{E_s e_s + E_f e_f}\right) \frac{F}{b} - \frac{\nu_f}{E_f}(\sigma_{11}^{rf} + \sigma_{22}^{rf}) + \ln\left(\frac{1}{\sin\theta_0}\right), \quad (4)$$

$\nu_f$  is the thin film Poisson's ratio; the A (resp. r) index refers to the applied (resp. residual) stresses. Plotting  $P_1^f$  versus the applied force  $F$ , we obtain a linear curve. Its slope is  $P^*$

$$P^* = \frac{1}{b} \left(\frac{1 + \nu_f}{E_s e_s + E_f e_f}\right). \quad (5)$$

Similarly, the curve of  $m_1^f$  vs  $F$  is linear; its slope  $m^*$  is

$$m^* = \frac{1}{b} \left(\frac{-\nu_f}{E_s e_s + E_f e_f}\right), \quad (6)$$

then we can deduce the Young's modulus  $E_f$  of the thin film from the sum of  $P^*$  and  $m^*$ , only knowing the substrate Young's modulus  $E_s$ :

$$E_f = \frac{1}{e_f} \left(\frac{1}{b(P^* + m^*)} - E_s e_s\right), \quad (7)$$

and its Poisson's ratio by a simple combination of these two experimental data without any other information on the substrate nor on the film

$$\nu_f = \frac{-m^*}{P^* + m^*}. \quad (8)$$

Furthermore, the combination of the "intersection method"<sup>4,5</sup> and this analytical method also extracts the substrate Poisson's ratio  $\nu_s$ :

$$\nu_s = \frac{\nu_f - \sin^2\psi_0^f}{\nu_f(1 - \sin^2\psi_0^f)}, \quad (9)$$

where  $\sin^2\psi_0^f$  is the abscissa of the intersection point of the thin film  $\sin^2\psi$  curves plotted for several loaded states. Here,  $\nu_f$  is the value deduced from Eq. (8).

The hypothesis of uniaxial stress state induces a much smaller error than one can imagine at first sight. In fact, the difference  $\Delta\nu = \nu_f - \nu_s$  between the Poisson's ratios of the thin film and the substrate induces a transverse applied stress  $\sigma_{22}^{Af} \approx \sigma_{11}^{Af} \cdot \Delta\nu$  while  $\sigma_{22}^{As} \approx 0$ .

Equation (3) becomes

$$\sigma_{11}^{Af} = \frac{F}{b \left(e_f + e_s \frac{E_s}{E_f} (1 - \nu_f \Delta\nu)\right)}, \quad (10)$$

which results in

$$P^* = \frac{1 + \nu_f}{b[E_f e_f + E_s e_s (1 - \nu_f \Delta\nu)]} \quad (11)$$

and

$$m^* = \frac{-\nu_f(1 + \Delta\nu)}{b[E_f e_f + E_s e_s (1 - \nu_f \Delta\nu)]}. \quad (12)$$

Finally, the film modulus calculated under a biaxial stress state ( $E_{f(bi)}$ ) can be estimated by

$$E_{f(bi)} = (1 - \nu_f \Delta\nu) \frac{1}{e_f} \left(\frac{1}{b(P^* + m^*)} - E_s e_s\right)$$

$$= (1 - \nu_f \Delta\nu) E_{f(uni)}, \quad (13)$$

where  $E_{f(uni)}$  is the film modulus calculated under uniaxial stress state [Eq. (7)]. Consequently, it is sufficient to measure the Young's modulus under the uniaxial stress hypothesis and then correct the obtained value by means of Eq. (13).

A 140 nm thick tungsten film was deposited on a 127.5  $\mu\text{m}$  thick polyimide (Kapton®) dogbone substrate by ion beam sputtering at room temperature. It was then submitted to an  $\text{Ar}^{2+}$  ion irradiation (340 keV–7.10<sup>14</sup> ions/cm<sup>2</sup>) to improve its crystalline quality.<sup>9</sup> The in-plane sample dimensions were 8×3 mm<sup>2</sup>. Tungsten was chosen because of its isotropic mechanical behavior and its high x-ray scattering factor. The external load was applied by means of a 300 N Deben™ tensile module. This tensile tester is equipped with a 75 N load cell enabling the force measurement with a precision higher than 0.1 N; it can be easily fitted to most goniometers thanks to its small volume (90×60×30 mm<sup>3</sup>) and low weight (350 g). Because of the low film thickness and small grain size ( $\geq 10$  nm), x-ray diffraction measurements were performed using a four-circle goniometer on the H10 beam line at the French synchrotron radiation facility LURE (Orsay, France). A large wavelength ( $\lambda = 0.2248$  nm) was chosen to analyze  $\{211\}$  family tungsten planes for each applied load.

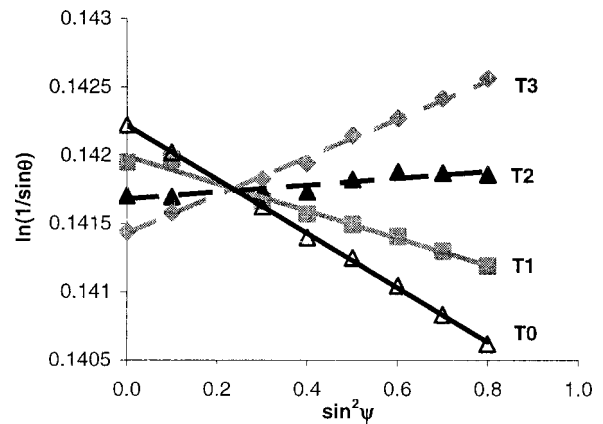


FIG. 2.  $\sin^2\psi$  curves relative to the  $\{211\}$  planes of the tungsten thin film in the unloaded state (T0) and for three progressive loading states (T1 to T3). The straight lines represent the linear regression on the experimental data. AIP license or copyright, see <http://ojps.aip.org/aplo/aplcr.jsp>

TABLE I. Slopes and intercepts of the  $\sin^2 \psi$  curves relative to the tungsten {211} family planes for four force values.

No. of the loading state	0	1	2	3
Applied force $F$ (N)	1.0	3.0	4.8	6.5
Slope $P_1^f$	-0.001 986	-0.001 001	0.000 254	0.001 408
Intercept $m_1^f$	0.142 221	0.141 993	0.141 681	0.141 424

The evolution of the  $\sin^2 \psi$  curves as a function of the applied load is shown in Fig. 2. T0 corresponds to the unloaded state while T1, T2, and T3 are related to increasing loading states. As assumed, these curves are linear. Their slope is directly related to the total stress in the film. The residual stresses are compressive; with increasing applied stress (from T1 up to T3), the total stress value decreases and then becomes tensile for T2 and T3. Table I presents the values of the applied force, the slope, and the intercept of the least-squared linear regression for each loaded state. Figure 3 shows the evolution of (a) the slope  $P_1^f$  and (b) the origin ordinate  $m_1^f$  of the  $\sin^2 \psi$  curves versus the applied force  $F$ . As predicted by Eq. (4),  $P_1^f$  and  $m_1^f$  depend linearly upon  $F$ . The slopes are, respectively,  $P^* = 6.2324 \times 10^{-4}$  and  $m^*$

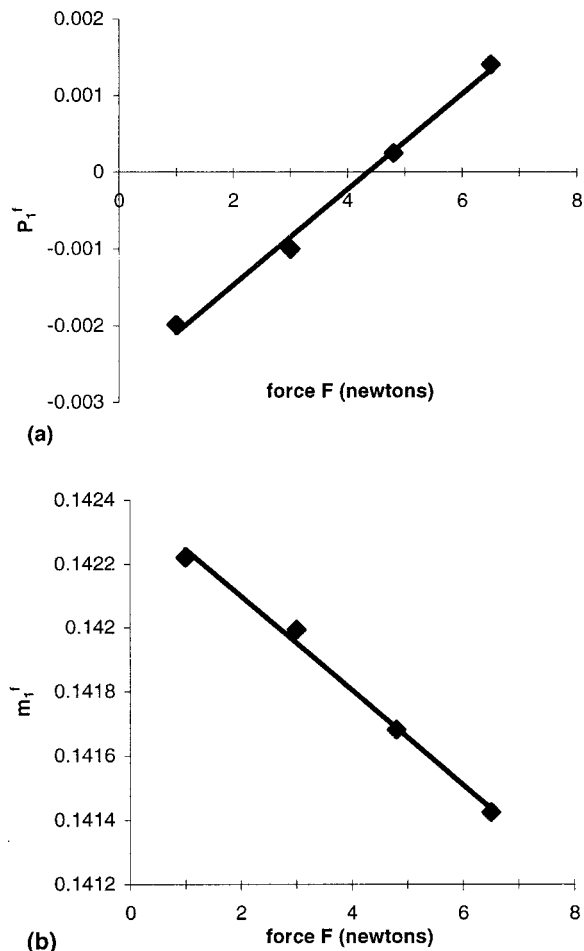


FIG. 3. Slope  $P_1^f$  (a) and intercept  $m_1^f$  (b) of the  $\sin^2 \psi$  curve vs the applied force  $F$  for four increasing loading states. The straight lines represent the linear regression on the experimental data; their slopes allow one to calculate  $E_f$  and  $\nu_f$ .

$= -1.4733 \times 10^{-4}$ . Having previously found by direct measurement the value of 5.17 GPa for the substrate Young's modulus, Eq. (7) leads to a value of  $390 \pm 40$  GPa for the thin film Young's modulus ( $E_f$ ), very close to the tungsten bulk value (388 GPa).<sup>10</sup> The film Poisson's ratio deduced from Eq. (8) is  $\nu_f = 0.310 \pm 0.015$ , which is significantly larger than the bulk value (0.284).

It should be noted that, since tungsten is elastically isotropic, the measurement of  $E_f$  and  $\nu_f$  allows one to calculate the thin film stiffness constants  $C_{11}$ ,  $C_{44}$ , and  $C_{12}$ . The obtained values are  $C_{11} = 541$  GPa,  $C_{44} = 149$  GPa, and  $C_{12} = 243$  GPa, while the literature values for bulk tungsten are, respectively, 501, 151, and 198 GPa.<sup>10</sup> We can observe that an increase of  $\nu_f$  (with a constant  $E_f$ ) results in a decrease of  $C_{11}$  and  $C_{12}$  whereas  $C_{44}$  remains unchanged. This is an important result which shows the advantage of the method used in this study; an interpretation in terms of microstructure modification and interatomic potentials constitutes other work and is still in progress. Finally, we can extract the Poisson's ratio of the Kapton® substrate thanks to Eq. (9). As can be seen in Fig. 1, all the  $\sin^2 \psi$  curves present a common intersection point where the abscissa ( $\sin^2 \psi_0^f$ ) is equal to 0.235. This leads to  $\nu_s = 0.312$ . We can then estimate the "biaxial correction" for the tungsten Young's modulus: according to Eq. (13),  $E_{f(\text{bi})}/E_{f(\text{uni})} = (1 - \nu_f \cdot \Delta \nu) = 1.0006$ . Consequently, the error committed here when assuming a uniaxial applied stress state is less than 0.1%. Thus it is perfectly justified to extract the thin film elastic constants in a very simple way under the uniaxial hypothesis.

In conclusion, an experimental technique for the determination of the Young's modulus and Poisson's ratio in thin films on substrates has been elaborated by combining x-ray diffraction strain measurements and *in situ* tensile testing. This method presents the following main advantages: (i) the unstrained lattice parameter of the film does not need to be known; (ii) no elastic constant of the substrate or the film is necessary to determine the Poisson's ratio of the film; and (iii) the only data needed to extract the Young's modulus of the film is the substrate Young's modulus. The precision will be improved thanks to an optimization of the sample dimensions. Currently we are engaged in the study of W sublayers in W/Cu multilayers to analyze the possible evolution of the W Young's modulus and Poisson's ratio when reducing the thickness period.

<sup>1</sup>H. Huang and F. Spaepen, *Acta Mater.* **48**, 3261 (2000).

<sup>2</sup>A. J. Kalkman, A. H. Verbruggen, and G. C. A. M. Janssen, *Appl. Phys. Lett.* **78**, 2673 (2001).

<sup>3</sup>J. Schjøtz, T. Vegge, F. D. Di Tolle, and K. W. Jacobsen, *Phys. Rev. B* **60**, 11971 (1999).

<sup>4</sup>P.-O. Renault, K. F. Badawi, L. Bimbault, Ph. Goudeau, E. Elkaim, and J. P. Lauriat, *Appl. Phys. Lett.* **73**, 1952 (1998).

<sup>5</sup>P.-O. Renault, K. F. Badawi, Ph. Goudeau, and L. Bimbault, *Eur. Phys. J.: Appl. Phys.* **10**, 91 (2000).

<sup>6</sup>P. Villain, P.-O. Renault, Ph. Goudeau, and K. F. Badawi, *Thin Solid Films* **406**, 185 (2002).

<sup>7</sup>C. Noyan and J. B. Cohen, *Residual Stress Measurement by Diffraction and Interpretation* (Springer, New York, 1987).

<sup>8</sup>V. Hauk, *Structural and Residual Stress Analysis by Nondestructive Methods: Evaluation, Application, Assessment* (Elsevier, New York, 1997).

<sup>9</sup>N. Durand, K. F. Badawi, and Ph. Goudeau, *J. Appl. Phys.* **80**, 5021 (1996).

<sup>10</sup>J. C. Smithells, *Metals Reference Book*, 5th ed. (Butterworths, London, 1976).